

Hands on Project: Large Photocathode PMT Characterization

Rickard Stroem*

Dept. of Physics and Astronomy, Uppsala University

E-mail: rickard.strom@physics.uu.se

Osamu Takachio†

Institute of Cosmic Ray Research, University of Tokyo

E-mail: takachio@km.icrr.u-tokyo.ac.jp

Aldo Ianni

I.N.F.N. Gran Sasso Laboratory

E-mail: aldo.ianni@lngs.infn.it

Oleg Smirnov

Joint Institute for Nuclear Research

E-mail: oleg.smirnov@lngs.infn.it

A series of measurements have been performed on a HQE 20-inch PMT in the Borexino PMT test facility at Gran Sasso. These PMTs will likely be used in the next-generation of large neutrino detectors, such as e.g. JUNO. We characterized the PMTs response to single electrons, the transit time spread, the dark rate and the amount of after pulsing and compared with the specifications from the manufacturer as well as with the PMTs used in the Borexino experiment. Our studies show that this type of PMT is well suitable for the next-generation of detectors but the effect of the Earth Magnetic field needs to be taken into account.

*Gran Sasso Summer Institute 2014 Hands-On Experimental Underground Physics at LNGS - GSSI14,
22 September - 3 October 2014
INFN - Laboratori Nazionali del Gran Sasso, Assergi, Italy*

*Speaker.

†Speaker.

1. Introduction

The next-generation of neutrino detectors are already being planned and tested, e.g. LBNE (Long Baseline Neutrino Experiment), LENA (Low Energy Neutrino Astronomy), JUNO (Jiangmen Underground Neutrino Observatory [3]) and Hyper-Kamiokande. To reach higher sensitivities these are all very large detectors in size and need inexpensive PMTs with high quantum efficiency as well as the biggest possible optical coverage. JUNO is mainly designed to study the neutrino mass hierarchy and to precisely measure three of the neutrino oscillation parameters. The current plan is to use $\sim 15,000$ HQE 20-inch PMTs to reach an optical coverage of $\sim 80\%$ [3].

We performed measurements on a HQE 20-inch PMT produced by HAMAMATSU (R3600-02 MOD venetian blind dynode with a total gain of 10^7 , HQE: 33.4 % at 400 nm [4], serial nr: ZP0029) at the PMT testing facility built for the Borexino experiment at LNGS (Laboratori Nazionali del Gran Sasso). In particular we studied the following characteristics: single photoelectron response (using ADC), transit time (sampling 100 ns using TDC with 250 ps resolution), dark rate (using scaler, i.e. counter) and after pulsing (sampling 30 μ s using multihit TDCs with 1 ns resolution).

2. Test facility

The test facility was originally built for the testing of PMTs used by the Borexino experiment but has also been used for more general PMT R&D. The facility consists of two adjacent rooms: one room with the electronic systems, one dark room where PMTs are mounted. The latter room also has an advanced system of magnetic coils that can be used to e.g. cancel out (to less than 10 % remaining non-uniformity) the effect of the Earth's magnetic field (EMF) that potentially can have a degrading effect on the PMT performance, see [2].

Laser light is sent to the PMT through optical fibers ending at a diffuser¹. The signals detected by the PMT goes through a Leading Edge Discriminator (LED) set at the level of 0.05 - 0.1 p.e. (photoelectron) and the surviving signals are fed into a Majority Logic Unit (MALU). The laser trigger is used as the majority external gate. The signals are amplified and subsequently fed to: Analog-to-Digital-Converter (ADC), Scaler (counter), Time-to-Digital-Converter (TDC), Multi-Time-to-Digital-Converter (multihit TDC, MTDC). For time signals we use a Constant Fraction Discriminator (CFD) set to 0.2 p.e. The details of the electronics system are described in [2].

3. Measurements

3.1 Charge - Single Electron Response

The Single Electron Response (SER) of the PMT is important specially in large detectors because the PMT typically detect very few photons per event. The calibrated charge spectrum obtained with the ADC is presented in figure 1. It shows several features: A sharp peak at 0.0 p.e. with long tails at both positive and negative values (the so-called pedestal), a smooth Gaussian distribution around 1.0 p.e. The main Gaussian peak centered around 1.0 p.e. is identified as due

¹Note that the photons produced by the laser are very narrow in time. In particular they are much narrower than the expected transit time and transit time spread, i.e. the pulses from the laser can be regarded as a delta function in time and hence allow for precision measurements of the timing properties of the PMT.

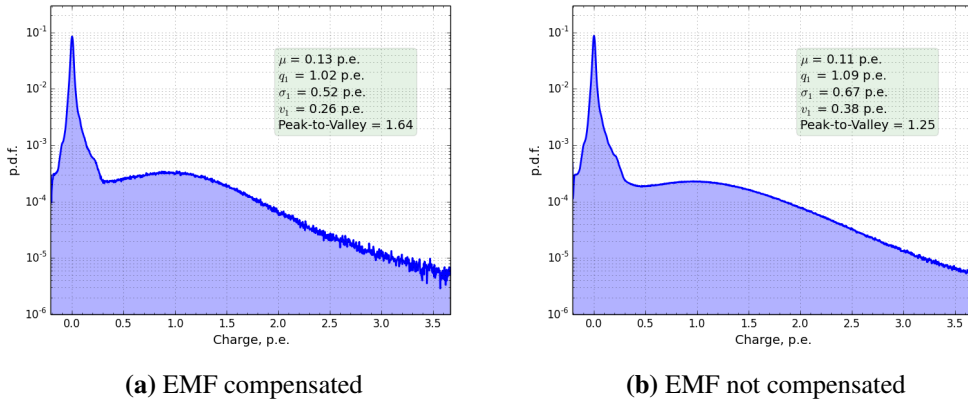


Figure 1: Charge spectrum. Calibrated ADC data is shown in blue. Left plot shows the characteristics with the EMF system activated, i.e. with compensation, while the right plot shows the situation when the system was deactivated, i.e. without compensation.

to single fully amplified photoelectrons while photoelectrons that are not fully amplified ends up in the pedestal part that can be described by an exponential with negative slope.

In figure 1 the charge histograms are shifted so that the pedestal position correspond to 0.0 p.e. This is done by fitting a Gaussian to the pedestal distribution and shifting the peak value to 0.0. The shift to non-zero values in raw data originates from a small DC offset between the output of the PMT and the input of the ADC. Further, the histograms are normalized to 1.

The probability to measure N events given a mean μ is given by the Poisson distribution: $P(N) = \frac{\mu^N}{N!} e^{-\mu}$. We extract the mean value μ of the SER through the relation $P(0) = N_{\text{ped}}/N_{\text{trig}} = e^{-\mu}$ where N_{ped} is the number of events with a photoelectron under the threshold 0.2 p.e. set by the CFD (ped = pedestal) and N_{trig} is the total number of single triggers.

The mean charge q_1 of the ideal SER (PMT response to 1 p.e.) is calculated using the equation $q_1 = Q/\mu$, where Q is the weighted mean charge of the charge histogram. σ_1 denotes the standard deviation of q_1 and the relative variance of the ideal SER ($v_1 = \sigma_1^2/q_1^2$) can be obtained by treating it as an extra noise factor: $(\sigma_Q/Q)^2 \approx (1+v_1)/Q$ where σ_Q^2 is the standard deviation of the weighted mean Q . The results of the calculations are presented in the boxes of figure 1 as well as in table 1.

In order to test whether the charge collection capabilities of the PMT is affected by the EMF we performed measurements both with and without the magnetic field compensation system. As can be seen by comparing figures 1a and 1b, the magnetic compensated spectrum has the desired property of smaller relative variance v_1 and larger peak-to-valley ratio.

The numerical results are presented in table 1 where we also have included values from two additional measurements, where the PMT was rotated along the symmetry axis about 90° .

3.2 Time Resolution

The photon arrival times at the PMTs are essential parameters for many experiments using either scintillation light or Cherenkov light to identify incoming particles. The times are used together with the deposited charge to determine several important properties of the incoming particle such as the position of the interaction vertex, the arrival direction, the energy and the particle type

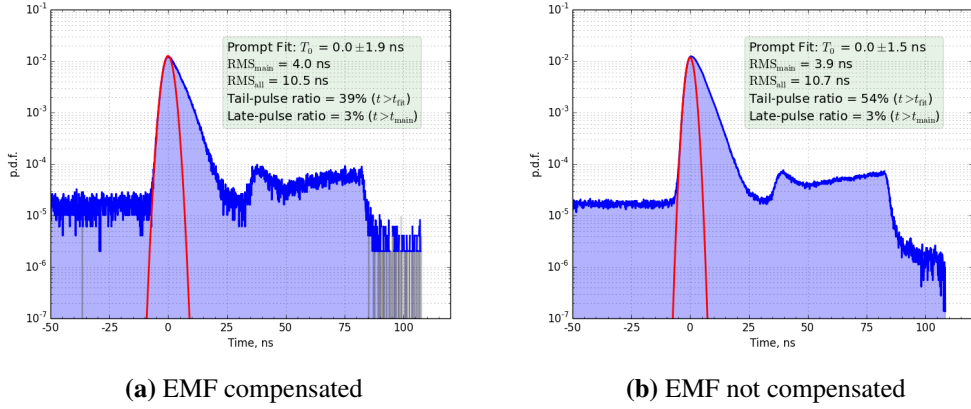


Figure 2: Transit time. Calibrated TDC data is shown in blue. The red line shows the Gaussian fit to the prompt peak. Left plot shows the characteristics with the EMF system activated, i.e. with compensation, while the right plot shows the situation when the system was deactivated, i.e. without compensation.

(through e.g. pulse shape α/β -discrimination). Further the precision in time is essential to disentangle coincident or near-coincident events. One of the most important properties of a PMT is hence a fast time response to incoming radiation, i.e. the so-called transit time, the time between the arrival of a photon at the photocathode and the electric burst at the anod, should be as small as possible. Even more important is to minimize the spread in transit time TTS (Transit Time Spread) between photoelectrons that formed on the same location of the photocathode.

In figure 2 we present the transit time pdfs. Each histogram is normalized and shifted so that the main prompt peak has its maximum at $t = 0$ ns. The timing distribution has several interesting features: the main peak centered at $t = 0$ ns (note the large tail towards longer times), the sharp peak at 40 ns, the broad distribution that reaches a maximum at about 80 ns, an uniform distribution of noise pulses present over the full range of times (describe in section 3.4).

The main peak is due to the prompt response of the PMT to incoming light and deviates largely from a Gaussian shape for both $t < 0$ and $t > 0$. The early pulses in this peak ($t < 0$) are likely due to elastic scattering of photoelectrons on the first dynode without multiplication [6], while the late pulses in this peak ($t > 0$) are due to inelastic scattering from the first dynode. We identify the sharp peak at 40 ns as due to light feedback on the accelerating dynode since the time difference corresponds approximately to the travel distance between the photocathode and the focusing grid. The peak at 80 ns is due to late pulses produced when the photoelectrons scattering elastically off the accelerating grid. The additional time of these pulses is approximately equal to double the time it takes for the electron to travel between the grid to the photocathode and back. The broad distribution that leads up to the peak at 80 ns is due to inelastic scattering of the photoelectron on the first dynode resulting in two pulses, of which one is slightly delayed due to the slightly lower energy that leads to a slower drift. Pre pulses, either due to electrons taking shortcuts in the multiplication (avalanche) region or photoproduction on the first dynode, are largely suppressed by discrimination thresholds and are not a visible feature in our measurements.

To characterize the PMT we studied the following parameters: width of the prompt peak

(determined by fitting a Gaussian to the $t < 0$ distribution), RMS of the full main peak, RMS of the distribution at $t > -10$ ns, fraction of tail pulses (pulses at $t > t_{full}$), fraction of late pulses $t > t_{main}$. The calculated quantities are presented in figure 2 as well as in table 1. The manufacturer measured the transit time FWHM of this PMT to be 6.2 ns. Hence the value we measured is somewhat higher: ~ 4 ns (FWHM $\approx 2.354\sigma$). As for the charge characterization we measured the timing properties of the PMT both with and without the magnetic field compensation (see table 1).

3.3 After Pulses

After pulses are artifacts in the PMT induced by true signal pulses. There delayed timing relative to the true signal pulse cause large problems, in particular for large detectors with many PMTs, since they can produce random triggers in the system providing a false event in coincidence with a real one. In general after pulses are thought to be due to rest gas in the PMT being ionized. These positively charged ions return to the photocathode inducing additional photoelectrons that go through the same chain of multiplication as the initial photoelectron that was induced by the incoming photon. We studied the ratio of the number of pulses in the time region between 400 ns and 28 μ s after each single photoelectron trigger to the total number of single triggers: $\sum N_{(400\text{ ns} < t < 28\text{ }\mu\text{s})} / \sum N_{\text{Single Trigger}}$. The after pulse fraction is about 3 % in both cases (w/ and w/o the EMF compensation). As a reference, the 8-inch PMT used in the Borexino experiment has an after pulse ratio of about 4.9 % on average [5].

3.4 Dark Rate

The PMT setup can trigger even in the absence of light, giving rise to a so-called dark rate (or dark noise): pulses randomly distributed in time. Since the surface material of the photocathode and dynodes typically have a low work function one main source of noise in room temperature is thermionic emissions, described by Richardson's Law [4]. Other sources of noise that are important when operating at high voltage (~ 1800 V) are: photocurrent from scintillations of the PMT construction material, electric field emission current and leakage current.

For detectors with many PMTs that operate in the single photoelectron regime (typical for low-background neutrino experiments) the dark rate causes similar problems as after pulses, i.e. it produces random coincidences that may trigger the system to cause false signals that interferes with true signals. Hence, the dark rate should be kept as low as possible. We define dark rate as being pulses that appear outside of the main characteristics of the time spectrum. The reference value for this PMT from the documentation from HAMAMATSU is a dark rate of about 19800 Hz if operated at 1900 V. The PMT in our setup operated at 1789 V and gave a dark rate of about 3300 Hz, hence much lower than the value from the manufacturer. The dark rate was measured several hours after it was put in complete darkness, in specific we did the measurements well after the fast component of the dark rate decayed (3-4 h [5]). It is also worth noting that the temperature at an underground facility like e.g. JUNO will be lower than in the Borexino test facility at LNGS, hence an even lower dark rate can be expected.

4. Conclusions

We have made several measurements to characterize a HQE 20-inch PMT likely to be used

Measurement	μ [p.e.]	q_1 [p.e.]	σ_1 [p.e.]	v_1 [p.e.]	P/V	TTS Main RMS [ns]
w/ EMF comp.	0.13	1.02	0.52	0.26	1.64	4.0
w/o EMF comp.	0.11	1.09	0.67	0.38	1.25	3.9
w/ EMF comp. 90°	0.13	1.02	0.53	0.26	1.52	4.0
w/o EMF comp. 90°	0.12	1.16	0.76	0.44	1.45	4.1

Table 1: Results from four measurements: PMT in original position with and without EMF compensation and two measurements where the PMT was rotated about 90° around its symmetry axis, again with and without EMF compensation. The dark rate measured (3300 Hz) is considerably lower than the value specified by the manufacturer. After pulse fraction is about 3 % for all measurements.

in the next-generation of large neutrino detectors. In particular we studied the PMTs response to single electrons, the transit time spread, after pulsing and the dark rate. Results are presented in figure 1 and 2 as well as in table 1. In addition to the measurements presented above, table 1 also includes results from two tests where the PMT was rotated along its symmetry axis about 90 degrees. Our tests show that the PMT is sensitive to the presence and possibly also the direction of the EMF. Hence experiments such as e.g. JUNO will have to compensate for this effect. Indeed current plans for the JUNO experiment includes using either built-in mu-metal shields (passive reduction of EMF) and/or huge Helmholtz coils surrounding the experiment (active cancellation of EMF).

References

- [1] G. Alimonti *et al.* [Borexino Collaboration], *The Borexino detector at the Laboratori Nazionali del Gran Sasso, Nucl. Instrum. Meth. A* **600** (2009) 568 [[physics/0806.2400](#)].
- [2] A. Brigatti, A. Ianni, P. Lombardi, G. Ranucci and O. Smirnov, *The Photomultiplier tube testing facility for the Borexino experiment at LNGS, Nucl. Instrum. Meth. A* **537** (2005) 521 [[physics/0406106](#)].
- [3] M. He [JUNO Collaboration], *Jiangmen Underground Neutrino Observatory*, [[physics/1412.4195](#)].
- [4] HAMAMATSU PHOTONICS K. K. *Photomultiplier Tubes: Basics and Applications*, Third Edition (Edition 3a), (2007).
- [5] A. Ianni, P. Lombardi, G. Ranucci and O. Smirnov, *The Measurements of 2200 ETL9351 type photomultipliers for the Borexino experiment with the photomultiplier testing facility at LNGS, Nucl. Instrum. Meth. A* **537** (2005) 683 [[physics/0406138](#)].
- [6] O. Ju. Smirnov, P. Lombardi, G. Ranucci, *Precision Measurements of Time Characteristics of ETL9351 Photomultipliers, Instrum. Experim. Tech.* **Vol 47, Nr. 1** (2004) 69.